Regional Polysterism in the GTP-Bound Form of the Human c-Ha-Ras Protein[†,‡]

Yutaka Ito,[§,||] Kazuhiko Yamasaki,[§,⊥] Junji Iwahara,[§,#] Tohru Terada,[§,#] Akihide Kamiya,[§,#] Mikako Shirouzu,[§,#] Yutaka Muto,[§] Gota Kawai,[§,▽,◇] Shigeyuki Yokoyama,[*,§,#] Ernest D. Laue,[△] Markus Wälchli,[○] Takehiko Shibata,[||] Susumu Nishimura,[▼,♦] and Tatsuo Miyazawa[▽,▲,●]

Department of Biophysics and Biochemistry, Graduate School of Science, The University of Tokyo, 7-3-1 Hongo, Bunkyo-ku, Tokyo 113, Japan, Laboratory of Cellular and Molecular Biology and Cellular Signaling Laboratory, The Institute of Physical and Chemical Research (RIKEN), 2-1 Hirosawa, Wako, Saitama 351-01, Japan, Faculty of Engineering, Yokohama National University, Tokiwadai, Hodogaya-ku, Yokohama 240, Japan, Department of Biochemistry, Cambridge Centre for Molecular Recognition, The University of Cambridge, Tennis Court Road, Cambridge CB2 1QW, U.K., Bruker Japan, 3-21-5 Ninomiya, Tsukuba Ibaraki 305, Japan, Biology Division, National Cancer Center Research Institute, 5-1-1 Tsukiji, Chuo-ku, Tokyo 104, Japan, Banyu Tsukuba Research Institute in Collaboration with Merck Sharp and Dohme Research Laboratories, Banyu Pharmaceutical Co., Ltd., 3 Ohkubo, Tsukuba, Ibaraki 300-33, Japan, and Protein Engineering Research Institute, 6-2-3 Furuedai, Suita, Osaka 565, Japan

Received February 7, 1997; Revised Manuscript Received May 14, 1997[⊗]

ABSTRACT: The backbone ^{1}H, ^{13}C, and ^{15}N resonances of the c-Ha-Ras protein [a truncated version consisting of residues 1−171, Ras(1−171)] bound with GMPPNP (a slowly hydrolyzable analogue of GTP) were assigned and compared with those of the GDP-bound Ras(1−171). The backbone amide resonances of amino acid residues 10−13, 21, 31−39, 57−64, and 71 of Ras(1−171)·GMPPNP, but not those of Ras(1−171)·GDP, were extremely broadened, whereas other residues of Ras(1−171)·GMPPNP exhibited amide resonances nearly as sharp as those of Ras(1−171)·GDP. The residues exhibiting the extreme broadening, except for residues 21 and 71, are localized in three functional loop regions [loops L1, L2 (switch I), and L4 (switch II)], which are involved in hydrolysis of GTP and interactions with other proteins. From the temperature and magnetic field strength dependencies of the backbone amide resonance intensities, the extreme broadening was ascribed to the exchange at an intermediate rate on the NMR time scale. It was shown that the Ras(1−171) protein bound with GTP or GTPγS (another slowly hydrolyzable analogue of GTP) exhibits the same type of broadening. Therefore, it is a characteristic feature of the GTP-bound form of Ras that the L1, L2, and L4 loop regions, but not other regions, are in a rather slow interconversion between two or more stable conformers. This phenomenon, termed a "regional polysterism", of these loop regions may be related with their multifunctionality: the GTP-dependent interactions with several downstream target groups such as the Raf and RalGDS families and also with the GTPase activating protein (GAP) family. In fact, the binding of Ras(1−171)·GMPPNP with the Ras-binding domain (residues 51−131) of c-Raf-1 was shown to eliminate the regional polysterism nearly completely. It was indicated, therefore, that each target/regulator selects its appropriate conformer among those presented by the "polysteric" binding interface of Ras. As the downstream target groups exhibit no apparent sequence homology to each other, it is possible that one target group prefers a conformer different from that preferred by another group. The involvement of loop L1 in the regional polysterism might suggest that the negative regulators, GAPs, bind to the polysteric binding interface (loops L2 and L4) of Ras and cooperatively select a conformer suitable for transition of the GTPase catalytic center, involving loops L1 and L4, into the highly active state.

The Ras proteins, 21 kDa low molecular mass guanine nucleotide-binding proteins, are important for cell proliferation, terminal differentiation, and other cellular events (*1*). Like other guanine nucleotide-binding proteins (*2*), Ras has a GTPase activity and cycles between an inactive GDP[1]-bound form (Ras·GDP) and an active GTP-bound form (Ras·GTP) (*3*, *4*). The cellular activities of Ras depend on several regions of the protein (*1*, *5*, *6*). In particular, residues 10−16, residues 32−40 ("effector region"), and residues 57−

[†] This work was supported in part by a Grant-in-Aid for Scientific Research from the Ministry of Education, Science and Culture, Japan (06404080) to S.Y., a Grant-in-Aid (Bio Media Program) from the Ministry of Agriculture, Forestry and Fisheries, Japan (BMP 97-VI-5) to S.Y., grants for the Biodesign Research Program from RIKEN to Y.I. and S.Y., and a grant from the BBSRC in the U.K. to E.D.L. The Cambridge Centre for Molecular Recognition is supported by the BBSRC and the Wellcome Trust.

[‡] Coordinates for the minimized averaged structure of Ras(1−171)·GDP have been deposited with the Brookhaven Protein Data Bank under accession code 1AA9.

* To whom correspondence should be addressed.

[§] The University of Tokyo.

[||] Laboratory of Cellular and Molecular Biology, RIKEN.

[⊥] Present address: Structural Biology Centre, National Institute of Bioscience and Human Technology, 1-1 Higashi, Tsukuba, Ibaraki 305, Japan.

[#] Cellular Signaling Laboratory, RIKEN.

[▽] Yokohama National University.

[◇] Present address: Department of Chemistry and Biotechnology, Graduate School of Engineering, The University of Tokyo, 7-3-1 Hongo, Bunkyo-ku, Tokyo 113, Japan.

[△] The University of Cambridge.

[○] Bruker Japan.

[▼] National Cancer Center Research Institute.

[♦] Banyu Pharmaceutical Co., Ltd.

[▲] Protein Engineering Research Institute.

[●] This author is deceased.

[⊗] Abstract published in *Advance ACS Abstracts,* July 1, 1997.

S0006-2960(97)00296-1 CCC: $14.00

61 are responsible for binding of the phosphate groups of GDP/GTP for GTP hydrolysis and for GTP-dependent interactions with downstream effector proteins.

It has been found that Ras·GTP directly binds to the c-Raf-1 protein kinase (*7*−*12*) and activates it to phosphorylate and activate the mitogen-activated protein kinase (MAP kinase) kinase (or MEK) (*13*, *14*). Phosphatidylinositol 3-kinase (PI3-kinase) has also been proposed to be one of the downstream effectors of Ras (*15*). It has also been found that Ras·GTP binds to RalGDS and RGL, which are guanine nucleotide exchange factors of Ral (Ral-GEFs), and actually activates the Ral-GEF-mediated signaling (*16*−*19*). Moreover, it is well-known that the GTPase activating proteins (GAPs), such as p120-GAP and NF1, also bind specifically to Ras·GTP and enhance its GTPase activity (*20*). Although these four families of Ras-binding proteins (Raf kinases, PI3-kinase, Ral-GEFs, and GAPs) have only very limited sequence homology with each other, all of them can bind primarily to the same interface of Ras·GTP, but not Ras·GDP.

For understanding how Ras·GTP can interact with the downstream effectors and GAPs through the same binding interface, structural studies are indispensable. Actually, X-ray crystallographic and NMR studies for C-terminal-truncated versions [Ras(1−171) and Ras(1−166) that consist of residues 1−171 and 1−166, respectively] and the full-length version [Ras(1−189)] of Ha-Ras protein, bound with either GDP or slowly hydrolyzable GTP analogues, have shown that the aforementioned residues, 10−16, 32−40, and 57−61, are all in loop regions (loops L1, L2, and L4, respectively) close to each other on the protein surface (*21*−*33*). By the X-ray crystallographic studies, the conformational differences between Ras·GDP and Ras·GTP were found mainly in loop L2 (switch I) and the region including loop L4 and helix α2 (switch II) (*23*−*26*). However, these "switch" regions take different conformations in the two crystals of GTP analogue-bound Ras, Ras(1−166)·GMPPNP (*23*, *24*) and Ras(1−171)·GMPPCP (*25*, *26*). In particular, four independent conformations were reported for Ras(1−171)·GMPPCP. Furthermore, intermolecular contacts between the effector region (switch I or loop L2) and the neighboring Ras molecules were found for both Ras(1−166)·GMPPNP and Ras(1−171)·GMPPCP in the crystals, which might have restricted or altered the conformation of the region. Therefore, NMR studies of the Ras·GTP in aqueous solution may be necessary for probing more details of the "dynamic" conformational differences between Ras·GDP and Ras·GTP.

In the previous NMR studies on the Ras proteins (Ha-Ras and N-Ras), the amino acid-selective isotope labeling method was mainly employed to investigate the structural difference between Ras·GDP and Ras·GTP in aqueous solution (*34*−*48*). In the present study, we applied the uniform $^{13}C/^{15}N$-labeling and triple-resonance NMR techniques (*49*) and assigned the backbone ^{1}H, ^{13}C, and ^{15}N resonances of both Ras(1−171)·GDP and Ras(1−171)·GMPPNP, in order to examine all the amino acid residues of Ras in terms of conformational differences between the inactive and active forms.

MATERIALS AND METHODS

Protein Expression and Cell Growth. The *Escherichia coli* strain TG1 was transformed with the expression vector pRGH (*50*), encoding the first 171 residues of the human c-Ha-Ras protein. The unlabeled and uniformly ^{15}N-labeled Ras(1−171) proteins were obtained by growing bacteria at 37 °C in M9 minimal media as described previously (*34*, *41*). The uniformly ^{13}C- and $^{13}C/^{15}N$-labeled Ras(1−171) samples were prepared in the same conditions as uniformly ^{15}N-labeling except for the D-glucose concentration in the M9 medium (2 g of [$^{13}C_6$]-D-glucose/L). At a turbidity of about 1.0 A_{600} unit, protein expression was induced by the addition of 50 mg/mL indoleacrylic acid. The cells were harvested after the turbidity reached a plateau level and stored at −80 °C.

Protein Purification. All procedures for the protein preparation described below were performed at 4 °C. The cells were washed once, harvested, and resuspended to 0.1 g of cell paste/mL with the lysis buffer (50 mM Tris-HCl, pH 7.5, 1 mM PMSF, 0.01% Nonidet P-40, and 25% sucrose). The cells were lysed with lysozyme (0.1 mg/mL) for 15 min, and then the solution was stirred with DNase I (0.1 mg/mL), 0.5% Nonidet P-40, and 5 mM $MgCl_2$ for 15 min. The soluble and insoluble fractions were separated by centrifugation at 30000*g* for 30 min. The supernatant was loaded onto a DEAE-Sephacel (Pharmacia) anion-exchange column preequilibrated with the preparation buffer (50 mM Tris-HCl, pH 7.5, 1 mM DTT, 1 mM PMSF, and 1 mM $MgCl_2$). The protein was eluted using a 50−350 mM KCl gradient. Next, the crude protein solution was concentrated using a centriprep 10 concentrator (Amicon) and loaded onto a Sephadex G-75 Superfine (Pharmacia) gel-filtration column and then eluted with the preparation buffer. The fractions containing the protein was concentrated again using a centricon 10 (Amicon) concentrator. Finally, the protein solution was loaded onto a Mono-Q FPLC (Pharmacia) anion-exchange column and eluted using a 0−350 mM KCl gradient. The final sample was stored at −20 °C in 50% glycerol.

Preparation of the GTP-Bound Forms of Ras(1−171). In order to prepare the GTP-bound form and to avoid GTP hydrolysis during multidimensional NMR measurements, we used GMPPNP, a slowly hydrolyzable GTP analogue. Ras(1−171)·GTP and Ras(1−171)·GTPγS samples were also prepared for measurements of 2D $^{1}H-^{15}N$ HSQC spectra. To prepare these "GTP-bound" forms of Ras(1−171), the bound GDP was replaced by GMPPNP, GTP, or GTPγS, through incubation of the purified Ras(1−171)·GDP (0.5 mM) three times with the triphosphate nucleotide (2 mM) in the presence of 10 mM EDTA for 10 min at 37 °C. For the preparation of Ras(1−171)·GMPPNP, 10 units/mL apyrase (Sigma, Grade VI) was added to the incubation mixture in order to hydrolyze the released GDP molecules.

[1] Abbreviations: Ras(1−166), a recombinant protein consisting of residues 1−166 of the human c-Ha-Ras protein; Ras(1−171), a recombinant protein consisting of residues 1−171 of the human c-Ha-Ras protein; Ras(1−189), a recombinant full-length human c-Ha-Ras protein (residues 1−189); GAP, GTPase activating protein; GEF, guanine nucleotide exchange factor; MAP kinase, mitogen-activated protein kinase; PI3-kinase, phosphatidylinositol 3-kinase; RBD, Ras-binding domain; CRD, cysteine-rich domain; GDP, guanosine 5′-diphosphate; GTP, guanosine 5′-triphosphate; GMPPNP, guanosine 5′-*O*-(β,γ-iminotriphosphate); GTPγS, guanosine 5′-*O*-(3-thiotriphosphate); DTT, dithiothreitol; EDTA, ethylenediaminetetraacetic acid; PMSF, phenylmethanesulfonyl fluoride; Tris, tris(hydroxymethyl)aminomethane; NMR, nuclear magnetic resonance; 2D, and 3D, two and three dimensional, respectively; HSQC, heteronuclear single-quantum correlation; NOE, nuclear Overhauser effect; NOESY, NOE spectroscopy.

Preparation of Protein Samples for NMR Spectroscopy. Protein samples were concentrated and dissolved in the NMR buffer (90% ^1H_2O and 10% ^2H_2O containing 20 mM $Na_2HPO_4-NaH_2PO_4$, pH 5.5, 150 mM NaCl, and 10 mM $MgCl_2$) using a centricon 10 concentrator. The final volume was 200 μL. For the 100% ^2H_2O samples, the concentrated solutions were lyophilized and dissolved in 200 μL of ^2H_2O.

NMR Spectroscopy. NMR experiments were performed for 2−3 mM samples on Bruker AMX600, ARX400, and DRX400 spectrometers under the same condition. All spectra were processed on a Silicon Graphics Indigo^2 computer using the Azara software package (Boucher, unpublished) using a two-dimensional maximum entropy algorithm (*51*). All of the spectra were analyzed with the combination of customized macroprograms on FELIX Version 2.3 software (BIOSYM Inc.).

Backbone Resonance Assignments. The backbone ^1H, ^{13}C, and ^{15}N resonance assignments for Ras(1−171)·GDP and Ras(1−171)·GMPPNP were achieved by analysis of the spin−spin connectivities in four types of 3D triple-resonance spectra, HNCA, HN(CO)CA, and HNCO (*48*, *52*) and HCACO (*53*), and also of the sequential backbone NOEs in the 3D ^{15}N-separated NOESY-HSQC spectra (*54*, *55*). The 3D HNCA, HN(CO)CA, and HNCO spectra were acquired with a total of 64 (t_1, ^{13}C) × 32 (t_2, ^{15}N) × 512 (t_3, ^1H_N) complex points for the $^{13}C/^{15}N$-labeled protein in 90% ^1H_2O/10% ^2H_2O. The 3D HCACO spectrum was acquired with a total of 32 (t_1, $^{13}C_\alpha$) × 32 (t_2, ^{13}CO) × 256 (t_3, $^1H_\alpha$) complex points for the ^{13}C-labeled protein in 100% ^2H_2O. The 3D ^{15}N-separated NOESY-HSQC spectra were acquired with a mixing time of 100 ms and a total of 100 (t_1, ^1H) × 32 (t_2, ^{15}N) × 512 (t_3, ^1H_N) complex points for the ^{15}N-labeled protein in 90% ^1H_2O/10% ^2H_2O. A probe temperature of 37 °C was used for these experiments.

Temperature and Magnetic Field Dependencies of the $^1H-^{15}N$ HSQC Spectra. A series of $^1H-^{15}N$ HSQC spectra were measured for the ^{15}N-labeled Ras(1−171)·GDP and Ras(1−171)·GMPPNP at probe temperatures of 20, 25, 30, 35, 40, and 45 °C with the AMX600 spectrometer. At 30 °C, another $^1H-^{15}N$ HSQC spectrum was measured with the DRX400 spectrometer. These 2D HSQC spectra were acquired with 256 (t_1, ^{15}N) × 1024 (t_2, ^1H_N) complex points.

Backbone Dynamics. 2D $^1H-^{15}N$ correlation spectra to determine the $\{^1H\}-^{15}N$ NOE, T_1, and T_2 values were recorded for the ^{15}N-labeled Ras(1−171)·GDP and ^{15}N-Ras(1−171)·GMPPNP essentially as described by Skelton *et al.* (*56*). The relaxation parameters were calculated with the DABRET program (Iwahara, unpublished).

The $^1H-^{15}N$ HSQC Spectra of Amino Acid Selectively ^{15}N-Labeled Ras(1−171)·GMPPNP in the Complex with the Ras-Binding Domain of c-Raf-1. The Gly and Asp/Asn selectively ^{15}N-labeled Ras(1−171) samples were prepared as described previously (*41*). The c-*raf*-1 gene (*57*, *58*) was provided by the Japanese Cancer Research Resources Bank (JCRB). The DNA fragment encoding the Ras-binding domain (RBD, residues 51−131) of human c-Raf-1 (*11*, *59*) was inserted into the *Nde*I/*Sal*I site of the expression vector pK7 (*60*). The unlabeled sample of the Raf-1 RBD was obtained by growing *E. coli* strain BL21(DE3) (*61*) transformed with the expression vector in the LB medium at 37 °C. Expression of the protein was induced by the addition of 1 mM isopropyl β-D-thiogalactoside. The cells were broken by sonication. The protein was purified from the soluble extract by cation-exchange chromatography [a CM-Toyopearl (TOSOH) column] followed by gel filtration [a Sephadex G-75 Superfine (Pharmacia) column]. Each of the Gly and Asp/Asn selectively ^{15}N-labeled Ras(1−171)·GMPPNP samples were mixed with the unlabeled c-Raf-1 RBD at a molar ratio of 1:1 and then concentrated and dissolved in the NMR buffer with a centricon 3 (Amicon) concentrator. The 2D $^1H-^{15}N$ HSQC spectra were acquired with 256 (t_1, ^{15}N) × 1024 (t_2, ^1H_N) complex points at 30 °C for these samples.

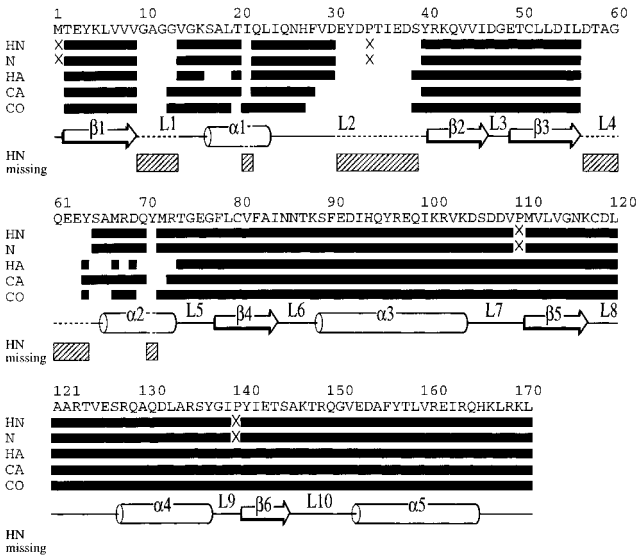

FIGURE 1: Schematic representation of the backbone sequence-specific assignment of Ras(1−171)·GMPPNP. The regions where backbone ^1H_N, ^{15}N, $^1H_\alpha$, $^{13}C_\alpha$, and ^{13}CO resonances were assigned are represented by horizontal bars. The ^1H_N and ^{15}N resonances of the N-terminal and three proline residues, which were not determined by the experiments we used, are represented by ×. The secondary structure of Ras(1−171)·GMPPNP determined by sequential NOEs, $^3J_{HNH\alpha}$ obtained by the HMQC-J experiment (*86*), and the amide−proton exchange rate obtained by $^1H-^2H$ exchange experiments is also shown.

RESULTS AND DISCUSSION

Assignments of the Backbone Resonances of Ras(1−171)·GDP. The backbone ^1H and ^{15}N resonances have been assigned nearly completely through 2D and 3D ^{15}N-separated NMR experiments performed on amino acid selectively or uniformly ^{15}N-labeled samples at 37 °C (*42*). In the present study, triple-resonance NMR experiments were performed to confirm the previous assignments and also to assign the backbone $^{13}C_\alpha$ and ^{13}CO resonances. By analysis of the four triple-resonance 3D NMR spectra, HNCA, HNCO, HN(CO)CA, and HCACO, of Ras(1−171)·GDP, we assigned all of the backbone ^1H, ^{13}C, and ^{15}N resonances, except for the ^{15}N resonances of the N-terminal methionine residue and the three proline residues.[2]

Assignments of the Backbone ^1H, ^{13}C, and ^{15}N Resonances of Ras(1−171)·GMPPNP. In a similar manner to that employed for Ras(1−171)·GDP, the backbone ^1H, ^{13}C, and ^{15}N resonances of most residues of Ras(1−171)·GMPPNP at 37 °C could be assigned (Figure 1).[2] However, it was

[2] The assignments of the backbone ^1H, ^{13}C, and ^{15}N resonances of both Ras(1−171)·GDP and Ras(1−171)·GMPPNP and the "missing cross peaks" phenomenon specific to Ras(1−171)·GMPPNP were reported by Y. Ito, Y. Muto, K. Yamasaki, G. Kawai, T. Miyazawa, M. Wälchli, S. Nishimura, and S. Yokoyama at the XVth International Conference on Magnetic Resonance in Biological Systems, Jerusalem, Israel, 1992.

found that 22 non-proline residues, 10−13, 21, 31−(Pro-34)−39, 57−64, and 71, give no detectable ^{1}H−^{15}N cross peaks in the 2D ^{1}H−^{15}N HSQC spectrum of Ras(1−171)·GMPPNP, whereas Ras(1−171)·GDP exhibits all of the backbone amide ^{1}H−^{15}N HSQC cross peaks as described above. We confirmed this interesting feature of Ras(1−171)·GMPPNP by measuring the ^{1}H−^{15}N HSQC spectra of 15 samples with different types of amino acid-selective ^{15}N-labeling [Ala, Ala/Val, Asp/Asn, Glu/Gln, Phe, Gly, Gly/Ser, His, Ile, Lys, Leu, Met, Arg, Val, and Tyr (*41*)] (data not shown). In summary, for Ras(1−171)·GMPPNP, we could not assign the resonances of 22 amide protons, 26 amide nitrogens (including proline residues), 32 α-protons, 25 α-carbons, and 27 carbonyl carbons (Figure 1).

Missing Backbone ^{1}H−^{15}N Cross Peaks of Ras(1−171)·GMPPNP. Thus, a surprisingly large number of ^{1}H−^{15}N HSQC cross peaks turned out to be missing. It was particularly interesting that the "missing cross peaks" phenomenon was presented specifically for the active GMPPNP-bound form of the Ras protein, but not for the inactive GDP-bound form, and that the residues of missing cross peaks are all from the functionally important regions involved in binding of the β- and γ-phosphate groups of GTP for GTP hydrolysis and for the interaction with downstream effectors and regulators (see Figure 2).[2] The disappearance of ^{1}H−^{15}N correlation cross peaks was reported in previous papers in which the amino acid-selective ^{15}N-labeling method was applied for glycine, isoleucine, and aspartate residues of N-Ras·GMPPNP and N-Ras·GTPγS (*44*−*46*) and also for glycine and serine residues of Ha-Ras(1−166)·GTPγS and Ha-Ras(1−166)·GMPPCP (*47*). They estimated regions for which ^{1}H−^{15}N cross peaks were missing in the GTP analogue-bound Ras by comparing the spectra with those of GDP-bound forms. In the present study, we finally identified all the missing cross peak residues by unambiguously assigning the backbone resonances of the observed ^{1}H−^{15}N cross peaks.

Temperature Dependency of the ^{1}H−^{15}N HSQC Spectra. It seemed that the "missing" cross peaks were too broad to be recognized. Some chemical exchange on the NMR time scale causes the dependency of the line shape on the exchange rate. Therefore, in order to examine if all or some of them were observable under different conditions, we first measured the 600/60.8-MHz ^{1}H−^{15}N HSQC spectra at 35, 40, and 45 °C for the uniformly ^{15}N-labeled Ras(1−171)·GMPPNP and Ras(1−171)·GDP. Figure 3 shows a region of each HSQC spectrum of Ras(1−171)·GMPPNP. In addition to the sequentially assigned cross peaks, three very broad cross peaks were observed at 45 °C (see the cross peaks indicated with boxes), indicating that their intensities are higher than those at 35 and 40 °C. This result strongly supported the idea of "intermediate" chemical exchange. We furthermore measured the ^{1}H−^{15}N HSQC spectra at lower temperatures, 30, 25, 20, and further down to 4 °C, but found that the exchange rate was still intermediate even at the lowest temperature (data not shown). Therefore, we could not find any conditions in which the exchange rate had been "slow" enough, on the NMR time scale, to exhibit two (or more) sets of separate cross peaks corresponding to the putative states in exchange. Next, for each of the resolved and assigned ^{1}H−^{15}N HSQC cross peaks of the uniformly ^{15}N-labeled Ras(1−171)·GMPPNP and Ras(1−171)·GDP at six different temperatures (20−45 °C), the intensity (the peak height) was measured and normalized relative to that at 35 °C (Figure 4). For Ras(1−171)·GDP, the intensities of all these cross peaks were only slightly increased when the temperature was raised from 20 to 45 °C. This was also the case for the majority of the cross peaks observed for Ras(1−171)·GMPPNP. By contrast, it was found that Ras(1−171)·GMPPNP exhibits stronger cross peaks at the higher temperature, for residues 8, 15−17, 19, 20, 23−25, 29, 46, 54, 56, 65, 66, 68−70, 72, 74, 76, 79, 81, 90, 93, and 95. It should be noted here that all of these residues are close to loop L1, L2, or L4 in the primary/tertiary structure.

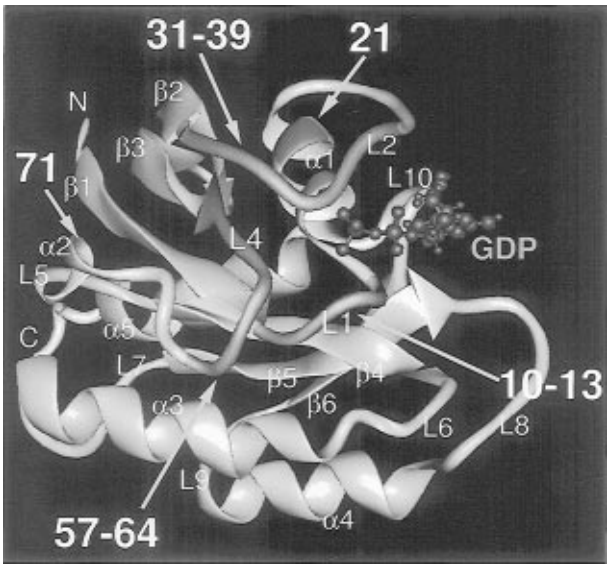

FIGURE 2: The distribution of regions in which ^{1}H−^{15}N correlation cross peaks were missing is colored in red on a ribbon model of the solution structure of Ras(1−171)·GDP determined by NMR spectroscopy. The GDP molecule is shown in blue. The detailed description of the side-chain resonance assignment and the structure determination steps will be published elsewhere. The structures were finally calculated using 2653 restraints consisting of 2381 NOE-derived distance restraints, 90 ϕ and 64 χ1 dihedral angle restraints, 118 hydrogen bond distance restraints, and additional 11 distance restraints derived from literature data defining interaction between the GDP, the magnesium ion, and the protein. We included similar literature-derived restraints as Kraulis *et al.* (*33*) used for the structure calculation of Ras(1−166)·GDP. Structures were calculated using the program X-PLOR Version 3.1 (*87*), employing an *ab initio* full simulated annealing protocol which starts from an extended strand (*88*). The root mean square (rms) deviations between the 30 final structures and the average structures are 0.61 Å for backbone atoms and 1.18 Å for all heavy atoms of residues 1−165. The C-terminal residues are disordered in the solution structure. The solution structures of Ras(1−171)·GDP and Ras(1−166)·GDP are almost identical except for several regions in which the structures were relatively ill-determined for both samples. The rms deviations between these solution structures are 2.09 Å for backbone atoms and 2.79 Å for all heavy atoms of residues 1−165.

Magnetic Field Dependencies of the ^{1}H−^{15}N Correlation Spectra. Then, we measured the ^{1}H−^{15}N HSQC spectrum of Ras(1−171)·GMPPNP (30 °C) at a lower field, 9.4 T (the ^{1}H frequency of 400 MHz), for comparison with that at 14.1 T (600 MHz) (Figure 5). Since magnetic field strength and frequency differences are proportional, the weaker the magnetic field strength becomes, the more line shape may sharpen. As expected, three additional cross peaks were observed at the 9.4 T spectrum (see the cross peaks indicated with boxes). As these three cross peaks appeared in the Gly resonance region, the HSQC spectra of the Gly selectively ^{15}N-labeled Ras(1−171) in the GMPPNP-bound form were measured at higher temperatures, 37 and 45 °C, at 9.4 T

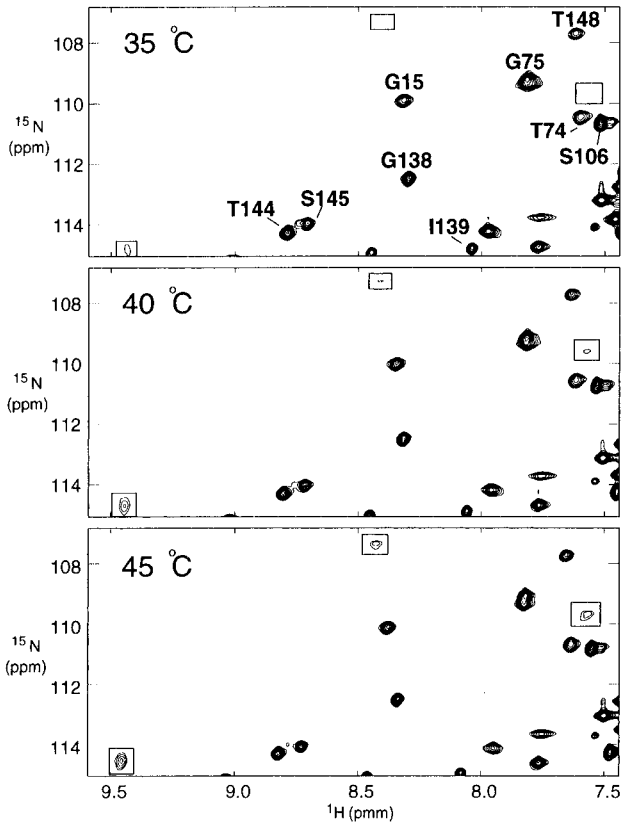

FIGURE 3: Contour plots of a region of $^{1}H-^{15}N$ HSQC spectra of Ras(1−171)·GMPPNP measured at three different probe temperatures (35, 40, and 45 °C). The assignment of each cross peak is shown in the spectrum at 35 °C.

(Figure 6). The three cross peaks were observed relatively well at 45 °C (see the cross peaks indicated with boxes in Figure 6) but could not be assigned sequentially because the protein was denatured more rapidly at 45 °C than at 37 °C. On the other hand, the spectra at 9.4 T/37 °C gave us sufficient sequential NOEs to assign another $^{1}H-^{15}N$ cross peak, which was extremely broadened at 14.1 T, to Ile-21. Then, for the two magnetic fields, 9.4 and 14.1 T, the intensities of all resolved and sequentially assigned cross peaks were obtained and normalized relative to that of the C-terminal residue, Leu-171, as shown in Figure 7. Again, several residues surrounding loops L1, L2, and L4 (residues 16, 29, 54, 68, 70, 72, 76, and 100) exhibited stronger cross peaks at 9.4 T than at 14.1 T.

"Regional Polysterism". From these temperature and magnetic field dependencies of the $^{1}H-^{15}N$ HSQC spectra, we concluded that the cross peaks of the residues in loops L1, L2, and L4 of Ras(1−171)·GMPPNP were extremely broadened because of a chemical exchange at an intermediate rate on the NMR time scale and were therefore unobservable under the conditions of 37 °C and 14.1 T. The intensities of the extremely broadened cross peaks were lower than the noise level, 0.05 of those of the normal cross peaks in the $^{1}H-^{15}N$ HSQC spectra. As the conversion rate is remarkably slow, the exchange is probably between two or more stable conformations of the loop regions. In contrast, the fluctuations or segmental motions of unstructured loops in proteins usually cause relatively sharper NMR signals than those from the protein core. We therefore distinguished the characteristic conformational multiplicity of Ras(1−171)·GMPPNP from the usual flexibility of loop regions and termed it "polysterism". In the present study, we examined the backbone resonances of Ras(1−171). It should be emphasized, therefore, that the present phenomenon is not restricted to side-chain conformations but is likely to involve stable backbone conformations along the loops. The polysterism of Ras(1−171)·GMPPNP is specifically localized in the regions consisting of residues 10−13 (loop L1), 21 (in the center of helix α1), 31−39 (the C-terminal half of loop L2 and a part of strand β2), 57−64 (loop L4), and 71 (in the center of helix α2). These regions are close to each other in the tertiary structure (Figure 2) and may concertedly function as an active site for the GTP hydrolysis and for the GTP-dependent interaction with the downstream effectors and regulators. Consequently, the relatively slow transition between the stable states might be ascribed to cooperative conformational rearrangements among the three loop regions and the phosphate groups. Two "polysteric" residues, Ile-21 and Tyr-71, are isolated from the other polysteric loops in the primary structure, but their side chains are likely to be involved heavily in the putative conformational rearrangements. As described above, several residues surrounding the polysteric residues exhibited temperature- and magnetic field-dependent broadenings. However, the degrees of exchange broadening, and therefore the chemical shift differences between the distinct states, of the surrounding residues are much smaller than those of the polysteric residues.

Comparison of the Backbone $^{1}H_N-^{15}N$ Chemical Shifts and Dynamic Parameters between Ras(1−171)·GDP and Ras(1−171)·GMPPNP. Figure 8 shows the differences in the backbone $^{1}H_N$ and ^{15}N chemical shifts between Ras(1−171)·GDP and Ras(1−171)·GMPPNP. The resonances most shifted upon GDP to GMPPNP exchange are distributed near the polysteric regions. We also analyzed the backbone dynamics of both Ras(1−171)·GDP and Ras(1−171)·GMPPNP, using the steady-state $\{^{1}H\}-^{15}N$ NOE and the longitudinal and transverse ^{15}N relaxation rates (T_1 and T_2, respectively) of each residue (*62*). The NOE, T_1, T_2, and T_1/T_2 values are plotted along the amino acid sequence in Figure 9. As in the case of Ras(1−166)·GDP (*33*), residues 27−32, 58−66, and 107−109 (loops L2, L4, and L7, respectively) of Ras(1−171)·GDP exhibit significantly rapid internal motions on the sub-nanosecond time scale. In contrast, in Ras(1−171)·GMPPNP, the ^{15}N T_2 values of residues 7, 8, 14, 56, 66, and 70, which are near the polysteric regions, are shorter than those of other residues, indicating contributions of slower internal motions. This may suggest that some of the residues surrounding the regions exhibiting the polysterism are somewhat directly involved in the putative conformational rearrangements between the polysteric states.

Comparison of the $^{1}H-^{15}N$ HSQC Spectra of Ras(1−171)·GDP, Ras(1−171)·GMPPNP, Ras(1−171)·GTPγS, and Ras(1−171)·GTP. We also measured the $^{1}H-^{15}N$ HSQC spectrum of Ras(1−171) bound with GTPγS, which is another slowly hydrolyzable analogue of GTP. Next, we tried to measure the $^{1}H-^{15}N$ HSQC spectrum of Ras(1−171)·GTP, where GTP is the natural substrate of the Ras GTPase activity. Actually, by measurement of an HSQC spectrum, it was found that about 60% of the prebound GTP molecules in the sample of Ras(1−171)·GTP had already been hydrolyzed to GDP during the sample preparation process. The decrease in the intensities of the Ras(1−171)·GTP cross peaks and the increase in those of the Ras(1−171)·GDP cross peaks were monitored during incubation for

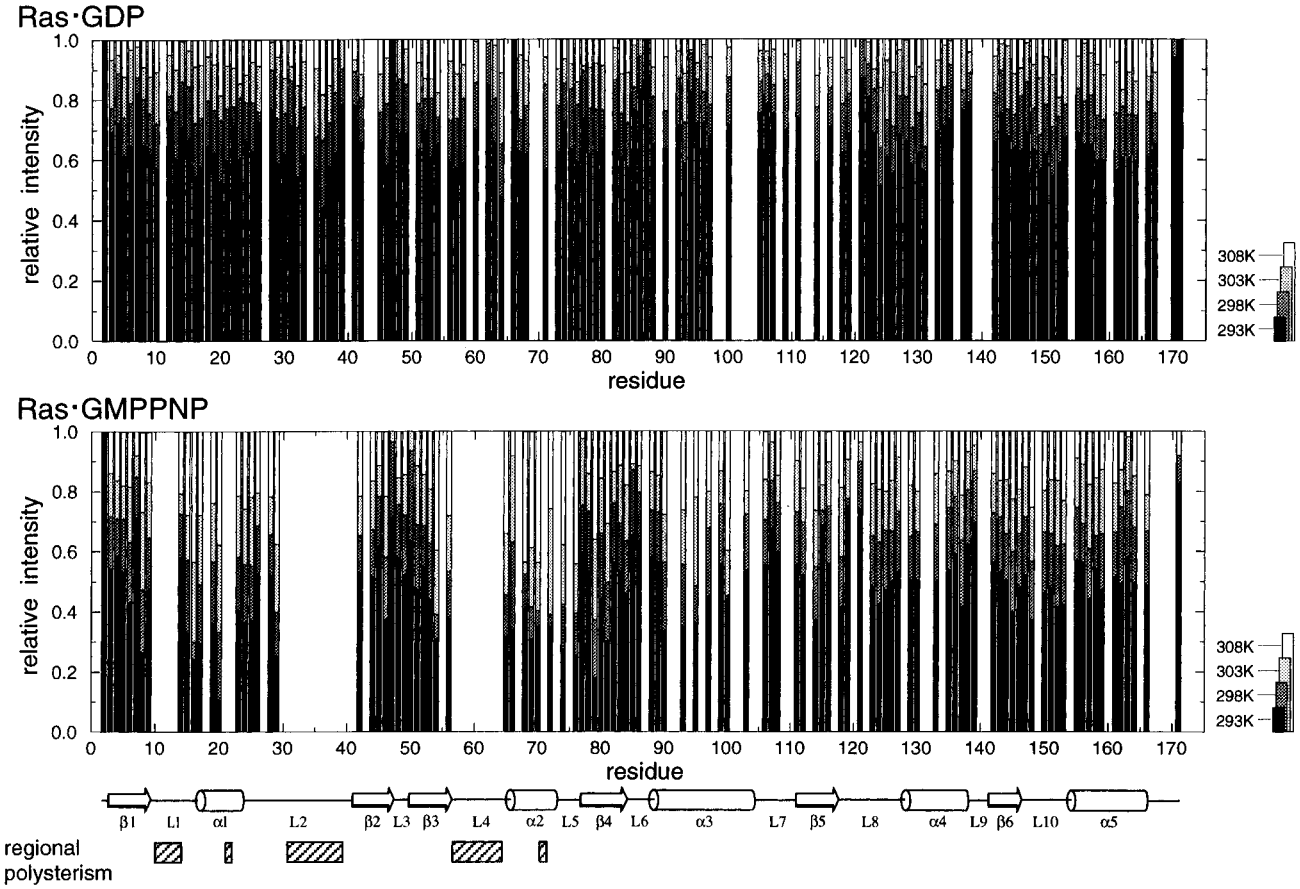

FIGURE 4: Plots of the temperature dependency of the $^1H-^{15}N$ cross peak intensity for observable cross peaks of Ras(1−171)·GDP and Ras(1−171)·GMPPNP. Data for overlapped cross peaks were excluded from these plots. The intensity of each cross peak was normalized relative to the intensity at 35 °C.

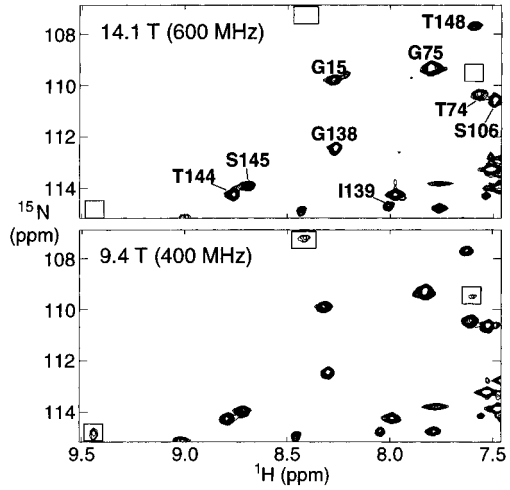

FIGURE 5: Contour plots of a region of $^1H-^{15}N$ HSQC spectra of Ras(1−171)·GMPPNP measured at 9.4 T (^1H frequency is 400 MHz) and 14.1 T (^1H frequency is 600 MHz). The three cross peaks that were observed at 9.4 T but not at 14.1 T are indicated by boxes.

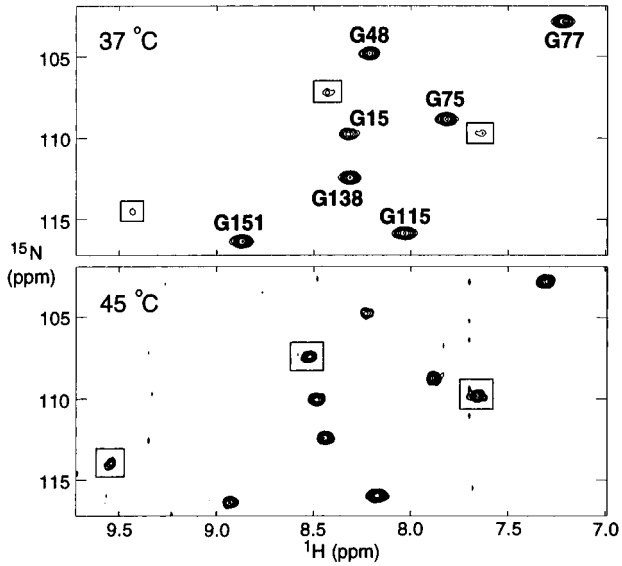

FIGURE 6: Contour plots of a region of $^1H-^{15}N$ HSQC spectra of Gly selectively ^{15}N-labeled Ras(1−171)·GMPPNP measured at two different probe temperatures (37 and 45 °C) at 9.4 T (^1H frequency is 400 MHz). The three cross peaks that showed temperature-dependent line broadening are indicated by boxes.

18 h at 25 °C; the population of Ras(1−171)·GTP was reduced by half approximately every 3 h. Thus, the "pure" HSQC spectrum of Ras(1−171)·GTP was obtained by subtracting the HSQC spectrum measured after the incubation for 18 h (GTP in the sample had mostly been hydrolyzed to GDP) from the spectrum that was initially measured before the incubation and corrected with the observed GTP:GDP ratio. Figure 10 shows a comparison of the $^1H-^{15}N$ HSQC spectra of Ras(1−171)·GDP, Ras(1−171)·GMPPNP, Ras-(1−171)·GTPγS, and Ras(1−171)·GTP. Two different regions (top and bottom) are shown.

In the HSQC spectra of Ras(1−171)·GTPγS and Ras(1−171)·GTP, cross peaks were observed exactly at, or very close to, the spectral positions corresponding to the cross peaks of Ras(1−171)·GMPPNP and were therefore assigned tentatively. In the Ras(1−171)·GTPγS spectrum, five or more cross peaks were additionally observed, which are four to five times broader than the normal cross peaks, while a

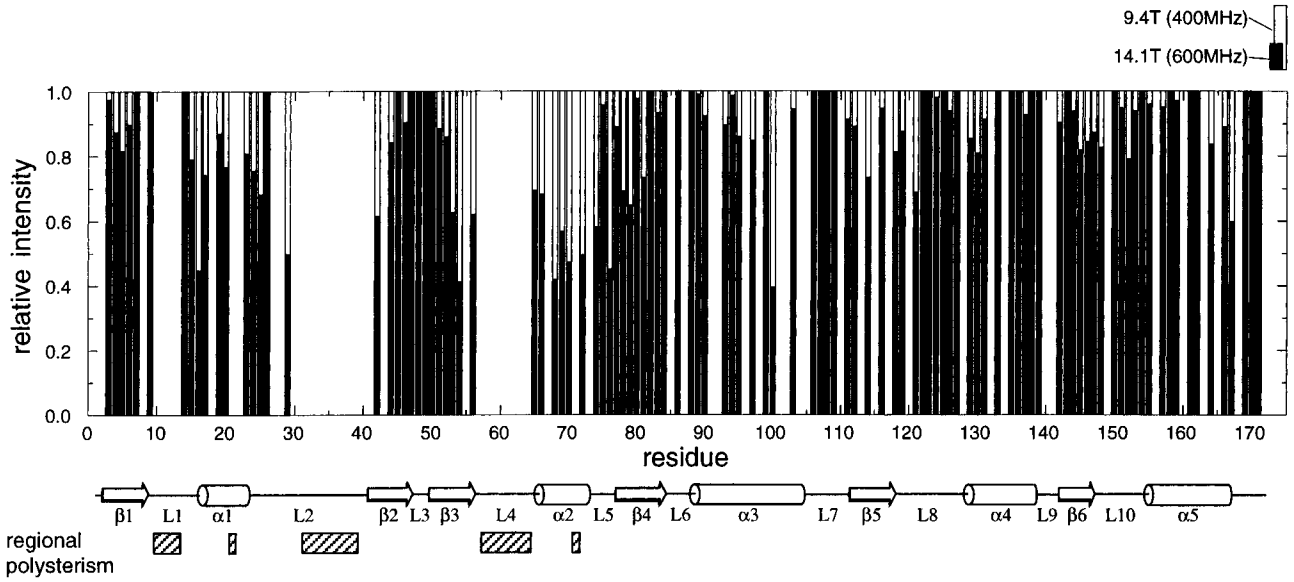

FIGURE 7: Plot of the magnetic field strength dependency of $^1H-^{15}N$ cross peak intensity for observable residues for Ras(1−171)·GMPPNP. Data for overlapped cross peaks were also excluded from these plots. In this plot the intensity of each cross peak was normalized assuming that the cross peaks of the C-terminal Leu-171 measured at 9.4 and 14.1 T show identical intensity.

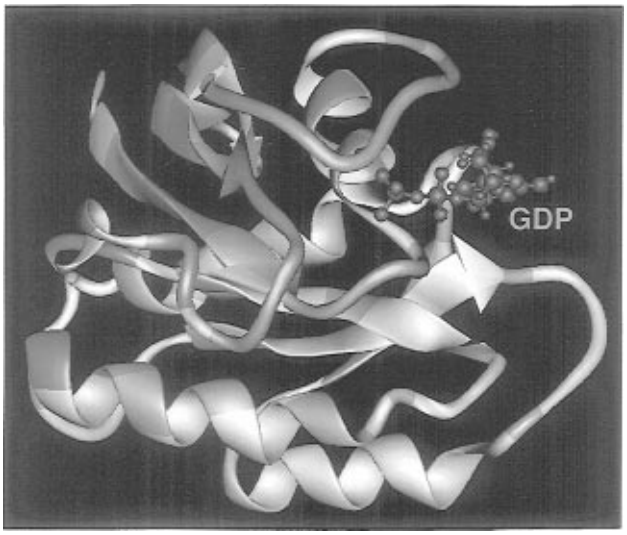

FIGURE 8: Chemical shift perturbation of backbone ^1H_N, ^{15}N, $^{13}C_\alpha$, and ^{13}CO nuclei upon GDP to GMPPNP exchange represented on the solution structure of Ras(1−171)·GDP. The residues whose backbone resonances were affected on the nucleotide exchange are displayed color coded. The mean shift difference Δ_{av} for each amino acid was calculated as $[(\Delta^1H_N)^2 + (\Delta^{15}N)^2 + (\Delta^{13}C_\alpha)^2 + (\Delta^{13}CO)^2]^{1/2}$, where Δ^1H_N, $\Delta^{15}N$, $\Delta^{13}C_\alpha$, and $\Delta^{13}CO$ are the chemical shift differences (Hz) between Ras(1−171)·GDP and Ras(1−171)·GMPPNP for resonances ^1H_N, ^{15}N, $^{13}C_\alpha$, and ^{13}CO observed at 14.1 T (the ^1H frequency is 600 MHz), respectively. The color coding is as follows: gray ($\Delta_{av} < 50$); light purple ($50 \le \Delta_{av} < 100$); light blue ($100 \le \Delta_{av} < 150$); green ($150 \le \Delta_{av} < 200$); yellow ($200 \le \Delta_{av} < 500$); and orange ($\Delta_{av} \ge 500$). The regions where the regional polysterism was found as the extreme line broadening of $^1H-^{15}N$ correlation cross peaks for Ras(1−171)·GMPPNP are shown in red. The GDP molecule is colored blue.

number of cross peaks are still missing under the noise level. For the Ras(1−171)·GTP spectrum, we found about 20 additional cross peaks, which are two to four times broader than the normal ones. These significantly broad $^1H-^{15}N$ cross peaks additionally observed for Ras(1−171)·GTPγS and Ras(1−171)·GTP probably correspond to those extremely broadened, and therefore unobservable, in the Ras(1−171)·GMPPNP spectrum. Moreover, several cross peaks, which were broadened but observable for Ras(1−171)·GMPPNP, exhibited increased heights in the Ras(1−171)·GTPγS and Ras(1−171)·GTP spectra (see the cross peaks indicated with boxes in Figure 10). All these results indicate that not only Ras(1−171)·GMPPNP but also Ras(1−171)·GTPγS and Ras(1−171)·GTP exhibit the characteristic regional polysterism localized in the same functional loop regions, while the rate of the putative conformational rearrangement slightly increases in the order of GMPPNP, GTPγS, and GTP. It is intriguing that the structural differences around the β- and γ-phosphate groups between GMPPNP, GTPγS, and GTP affect the conversion rate, which will be helpful in the future study on the nature of the conformational transition.

Comparison with the X-ray Crystallographic Studies. X-ray crystallographic studies on Ras(1−166)·GMPPNP and Ras(1−171)·GMPPCP have reported that the structural differences between the GDP- and GTP-bound forms are found mainly in the regions consisting of residues 30−38 (switch I) and 57−77 (switch II) (*23*−*26*). Note that these switch regions include loops L2 and L4, but not loop L1, among the three polysteric loop regions identified in the present study.

The conformations of the three loop regions (residues 10−13, 31−39, and 57−64), which are polysteric in solution, were well determined in the crystal structure of Ras(1−166)·GMPPNP, although residues 61−64 show relatively large thermal *B*-factors in the crystal (*23*, *24*). In this crystal structure of Ras(1−166)·GMPPNP, residues 12, 13, 32, 34, 61, 63, and 88 of one Ras(1−166) molecule are close (within 4 Å) to the effector region of another Ras(1−166) molecule; the side chain of Tyr-32 is in a hydrophobic intermolecular interaction and forms a hydrogen bond of its hydroxyl group with the γ-phosphate of GMPPNP bound to the neighboring Ras(1−166) molecule. These contacts in the crystal might have fixed the conformations of the loop regions, which are inherently polysteric.

In contrast, in the crystal of Ras(1−171)·GMPPCP, the four independent molecules exhibit different conformations in terms of the two switch regions (residues 30−38 and 59−73), depending upon their distinct intermolecular contacts. For example, the side chain of Tyr-32 of Ras(1−171)·

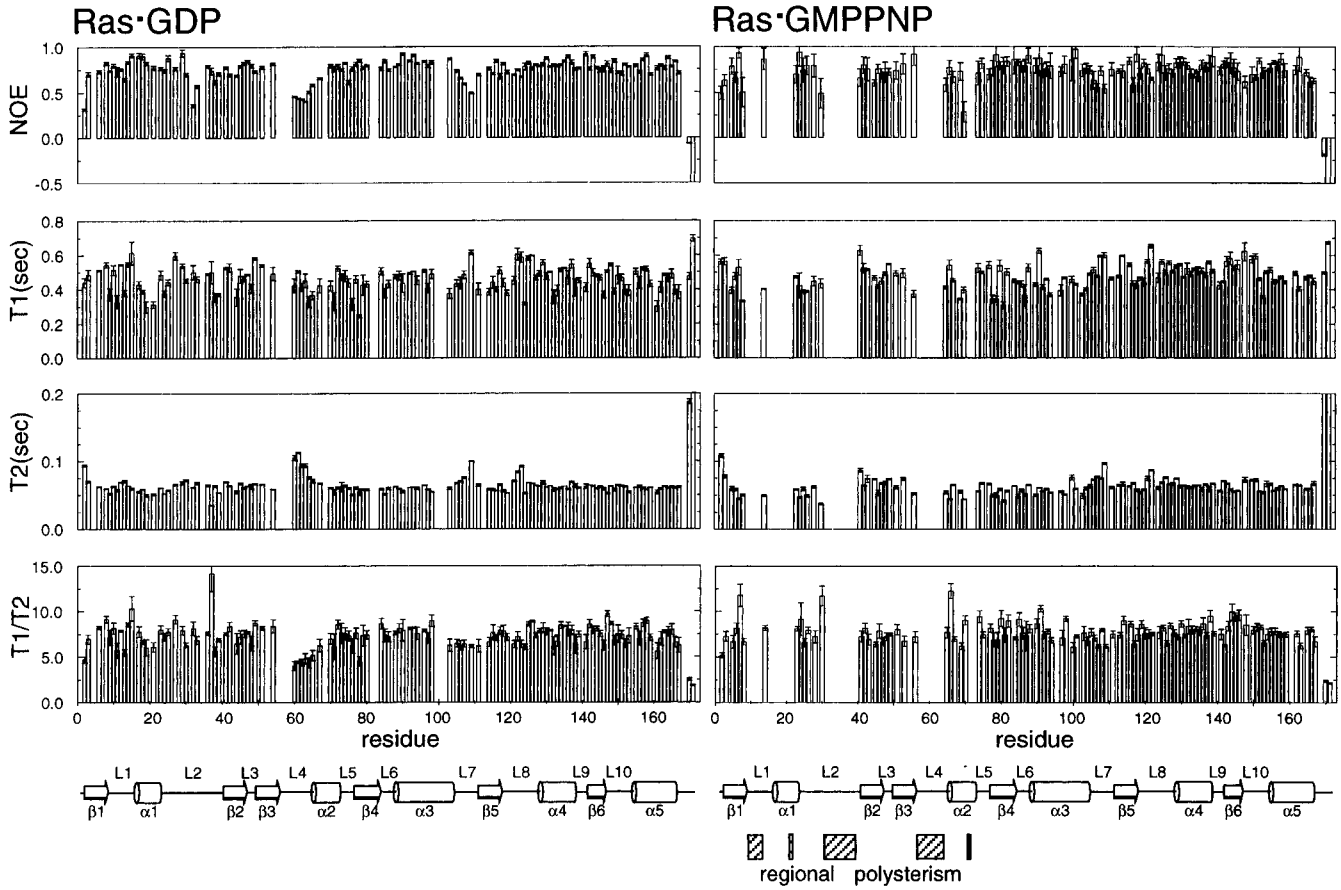

FIGURE 9: Plots of the $\{^1H\}-^{15}N$ NOE, ^{15}N T_1, T_2, and T_1/T_2 for observable backbone ^{15}N resonances for Ras(1−171)·GDP and Ras(1−171)·GMPPNP against the amino acid sequence. Data for overlapped cross peaks were excluded from these plots.

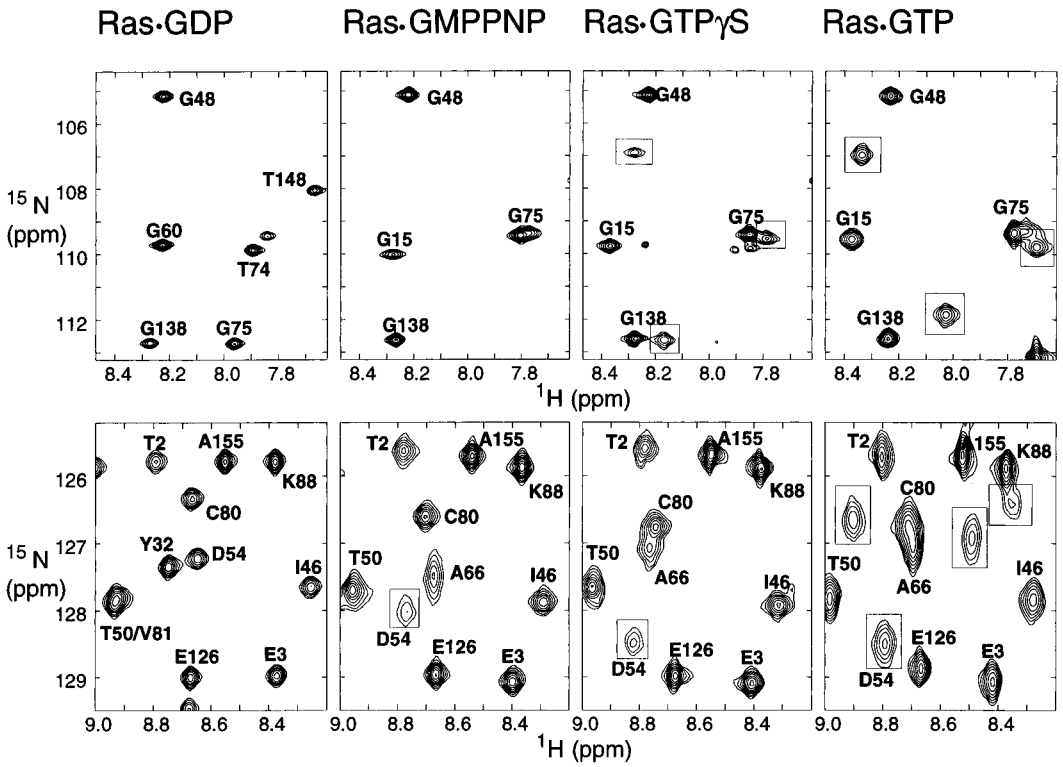

FIGURE 10: Contour plots of two different regions (top and bottom) of $^1H-^{15}N$ HSQC spectra of Ras(1−171)·GDP, Ras(1−171)·GMPPNP, Ras(1−171)·GTPγS, and Ras(1−171)·GTP. The spectra were measured at a probe temperature of 30 °C with the exception of that of Ras(1−171)·GTP which was measured at 25 °C. The cross peaks which showed significant difference in intensity between the spectra of Ras(1−171)·GMPPNP, Ras(1−171)·GTPγS, and Ras(1−171)·GTP are indicated by boxes.

GMPPCP forms intramolecular hydrophobic contacts with Ile-21, Ile-36, and Tyr-40 in two of the four conformers, as in the crystal structures of Ras(1−171)·GDP and Ras(1−189)·GDP (*21*, *22*, *29*), but points to the outside in the other

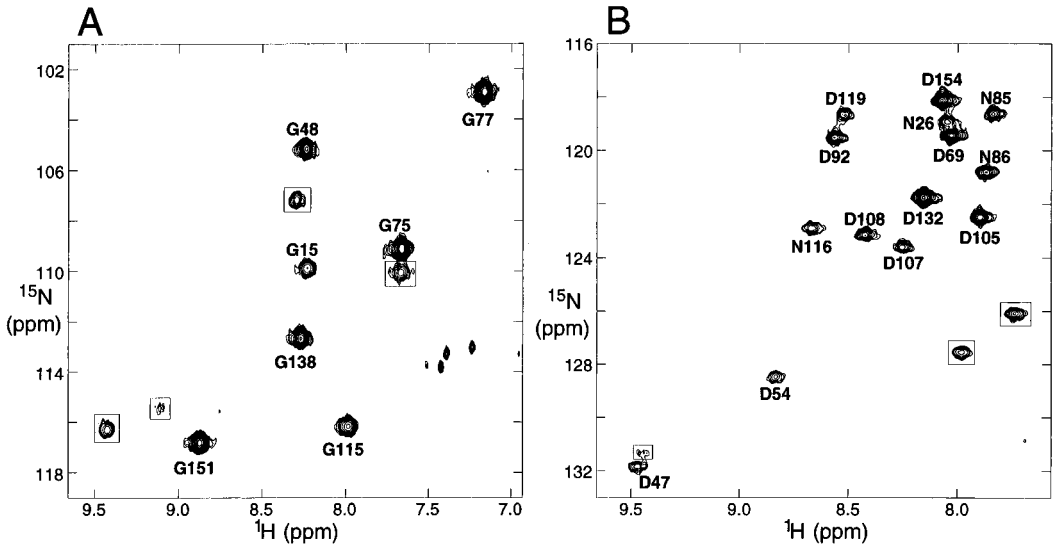

FIGURE 11: Contour plots of $^{1}H-^{15}N$ HSQC spectra of (A) Gly and (B) Asp/Asn selectively ^{15}N-labeled Ras(1−171)·GMPPNP in the complex with Raf-1 RBD. The cross peaks which were observed at positions similar to those for Ras(1−171)·GMPPNP were tentatively assigned. The seven (four for the Gly and three for the Asn/Asp selectively ^{15}N-labeled sample) cross peaks which were not observed for the Ras(1−171)·GMPPNP alone are indicated by boxes.

two conformers, as in the crystal structure of Ras(1−166)·GMPPNP (*23*, *24*). It is possible that these different conformations of the switch regions selected in the crystal are elements of the conformation set that characterizes the polysteric state of these regions of Ras in the GTP-bound form in solution.

The Regional Polysterism of Ras(1−171)·GMPPNP Was Significantly Reduced upon Binding with the Ras-Binding Domain of c-Raf-1. In order to examine how the regional polysterism of Ras(1−171)·GMPPNP is affected by upon complex formation with a downstream target, c-Raf-1, we measured the $^{1}H-^{15}N$ HSQC spectra of Gly and Asp/Asn selectively ^{15}N-labeled Ras(1−171)·GMPPNP in the complex with the Ras-binding domain (RBD, residues 51−131) of c-Raf-1 (*11*, *59*) (Figure 11). The cross peaks were observed at positions similar to those for the free state of Ras(1−171)·GMPPNP and could therefore be tentatively assigned. What should be emphasized is that seven cross peaks that were too broad to be detected for Ras(1−171)·GMPPNP by itself are clearly observed (four Gly and three Asn/Asp cross peaks) for Ras(1−171)·GMPPNP in the complex with the c-Raf-1 RBD. This finding indicates that the conformations of the polysteric loops of Ras(1−171)·GMPPNP are mostly fixed upon the RBD binding. It is strongly suggested that the conformations of the three loops are cooperatively interrelated in the presence of the γ-phosphate group, because the binding of the c-Raf-1 RBD fixes the conformations of not only the effector binding interface (loop L2 and possibly loop L4) but also the GTPase catalytic center (loops L1 and L4). The cross peak of an Asp/Asn residue is still "missing". In this context, it has been found that the Ras protein binds not only to RBD but also to the cysteine-rich domain (CRD) of c-Raf-1 (*63*−*67*). Consequently, the additional interaction of the c-Raf-1 CRD may fix the conformation of the cross peak-missing Asp/Asn residue, which is still polysteric in the complex of Ras(1−171)·GMPPNP only with the c-Raf-1 RBD. Consistently, the solution structures of the c-Raf-1 RBD (*68*, *69*) and CRD (*70*) in the absence of Ras have been found to exhibit no indication of polysterism unlike the GTP-bound form of Ras. The wild-type and mutant proteins of a Ras homologue, Rap1A, bound with GMPPNP and c-Raf-1 RBD are not polysteric in the crystalline state (*71*, *72*), while it has not yet been examined if Rap1A·GMPPNP has an intrinsic regional polysterism by itself in solution.

Relationship between the Regional Polysterism and Biological Functions of the Ras Protein. The finding of the regional polysterism characteristic to the GTP-bound form of Ras provides a possible mechanism of how Ras can interact properly with a variety of target groups, such as Raf kinases, Ral-GEFs, PI3-kinase, and GAPs, using its common binding interface, although these target groups exhibit no noticeable sequence homology to one another, except for the very weak homology between Raf and Ral-GEF RBD families (*73*). We now propose a hypothesis that a downstream target generally selects its favorite element among the conformer set presented by the polysteric regions of the GTP-bound form of Ras.

The interaction with GAPs significantly enhances the GTPase activity, whereas interactions with downstream effectors only enhance it slightly. Indeed, a recent report on the interaction between the Ras·GDP·AlF_4^- complex with GAPs or Raf-1 suggests that GAPs have an ability to stabilize an active conformation of Ras·GDP·AlF_4^- complex, while Raf-1 does not (*74*). The mechanism of the GTPase reaction has been investigated (*75*−*78*), but it has still been unclear whether some GAP residues contribute directly to the catalysis in the complex (*79*−*82*) or GAPs just stabilize a particular conformation that can express a very high GTPase activity of Ras (*77*). By replacing Gly-12 or Gly-13 by unnatural amino acids, it was suggested that loop L1 of the GTP-bound c-Ha-Ras can adopt two or more conformations in solution, and the switching between them is presumably important for the GAP-induced GTPase enhancement (*83*). The regional polysterism involving the three functional loops of Ras may indicate that the binding of GAPs selects one conformation of the binding interface and then cooperatively induces a transition of the conformation of the GTPase catalytic center into the highly active one.

When we were preparing this paper, a ^{31}P NMR study was reported, suggesting two conformational states around the phosphate groups of GMPPNP bound to Ras (*84*). The two conformational states are distinguished from each other only at 0 °C, and the large chemical shift difference of 0.7

ppm can be averaged out at higher temperatures (*84*). They concluded the two states are characterized by the different orientations of the Tyr-32 side chain (*84*). Their observations are coincident with ours, in particular, in the points that they proposed the existence of multiple (two in their report) conformations and the stabilization of one conformation by the complex formation with the Raf-1 RBD.

By simulating the contribution of the exchange to the ^{31}P line shapes, they calculated the exchange rates at various temperatures between the two states. Using their exchange rates and our experimental ^{15}N relaxation parameters for Ras(1−171)·GMPPNP, and supposing that the number of states of the regional polysterism is two, we simulated the ^{15}N line shapes via the Bloch equation by using the GAMMA Version 3.4 library (*85*). The minimum chemical shift differences that cause the reduction in the signal intensity down to the noise level were estimated to be around 500 Hz at 30 °C (exchange rate: 3421 Hz). It seems that such large chemical shift differences in ^{1}H and/or ^{15}N dimensions for all three polysteric loop regions may not be fully explained by the ring current shift proposed in the ^{31}P study (*84*). Furthermore, in the case of GTPγS binding, there is no indication of two conformational states in the ^{31}P spectra (*84*), while the extreme line broadening was found for ten and more ^{1}H−^{15}N HSQC cross peaks for Ras(1−171)·GTPγS in the present study. Accordingly, we would propose that the transition of the Tyr-32 side-chain conformation is a subprocess of the wider range regional polysterism process in the three functional loops, centering the γ-phosphate group.

ACKNOWLEDGMENT

We thank Dr. Brian Smith for numerous stimulating and enlightening discussions and for critical reading of the manuscript and Dr. Koji Takio for his help in the measurement on the AMX600 spectrometer in the Division of Biomolecular Characterization, RIKEN. Molecular graphics images were produced using the MidasPlus software from the Computer Graphics Laboratory, University of California, San Francisco.

SUPPORTING INFORMATION AVAILABLE

A list of backbone ^{1}H, ^{13}C, and ^{15}N resonance assignments for both Ras(1−171)·GDP and Ras(1−171)·GMPPNP at 37 °C, pH 5.5 (2 pages). Ordering information is given on any current masthead page.

REFERENCES

1. Barbacid, M. (1987) *Annu. Rev. Biochem. 56*, 779−827.
2. Kaziro, Y. (1978) *Biochim. Biophys. Acta 505*, 95−127.
3. Satoh, T., Nakamura, S., and Kaziro, Y. (1987) *Mol. Cell. Biol. 7*, 4553−4556.
4. Bourne, H. R., Sanders, D. A., and McCormick, F. (1991) *Nature 349*, 117−127.
5. Marshall, M. S. (1993) *Trends Biochem. Sci. 18*, 250−255.
6. Polakis, P., and McCormick, F. (1993) *J. Biol. Chem. 268*, 9157−9160.
7. Moodie, S. A., Willumsen, B. M., Weber, M. J., and Wolfman, A. (1993) *Science 260*, 1658−1661.
8. Zhang, X.-F., Settleman, J., Kyriakis, J. M., Takeuchi-Suzuki, E., Elledge, S. J., Marshall, M., S. Bruder, J. T., Rapp, U. R., and Avruch, J. (1993) *Nature 364*, 308−313.
9. Warne, P. H., Viciana, P. R., and Downward, J. (1993) *Nature 364*, 352−355.
10. Van Aelst, L., Barr, M., Marcus, S., Polverino, A., and Wigler, M. (1993) *Proc. Natl. Acad. Sci. U.S.A. 90*, 6213−6217.
11. Vojtek, A. B., Hollenberg, S. M., and Cooper, J. A. (1993) *Cell 74*, 205−214.
12. Koide, H., Satoh, T., Nakafuku, M., and Kaziro, Y. (1993) *Proc. Natl. Acad. Sci. U.S.A. 90*, 8683−8686.
13. Avruch, J., Zhang, X.-F., and Kyriakis, J. M. (1994) *Trends Biochem. Sci. 19*, 279−283.
14. Daum, G., Eisenmann-Tappe, I., Fries, H. W., Troppmair, J., and Rapp, U. R. (1994) *Trends Biochem. Sci. 19*, 474−480.
15. Rodriguez-Viciana, P., Warne, P. H., Dhand, R., Vanhaesebroeck, B., Gout, I., Fry, M. J., Waterfield, M. D., and Downward, J. (1994) *Nature 370*, 527−532.
16. Spaargaren, M., and Bischoff, J. R. (1994) *Proc. Natl. Acad. Sci. U.S.A. 91*, 12609−12613.
17. Hofer, F., Fields, S., Schneider, C., and Martin, G. S. (1994) *Proc. Natl. Acad. Sci. U.S.A. 91*, 11089−11093.
18. Kikuchi, A., Demo, S. D., Ye, Z.-H., Chen, Y.-W., and Williams, L. T. (1994) *Mol. Cell. Biol. 14*, 7483−7491.
19. Urano, T., Emkey, R., and Feig, L. A. (1996) *EMBO J. 15*, 810−816.
20. Bollag, G., and McCormick, F. (1991) *Annu. Rev. Cell Biol. 7*, 601−632.
21. de Vos, A. M., Tong, L., Milburn, M. V., Matias, P. M., Jancarik, J., Noguchi, S., Nishimura, S., Miura, K., Ohtsuka, E., and Kim, S.-H. (1988) *Science 239*, 888−893.
22. Tong, L., Milburn, M. V., de Vos, A. M., and Kim, S.-H. (1989) *Science 245*, 244.
23. Pai, E. F., Kabsch, W., Krengel, U., Holmes, K. C., John, J., and Wittinghofer, A. (1989) *Nature 341*, 209−214.
24. Pai, E. F., Krengel, U., Petsko, G. A., Goody, R. S., Kabsch, W., and Wittinghofer, A. (1990) *EMBO J. 9*, 2351−2359.
25. Brünger, A. T., Milburn, M. V., Tong, L., deVos, A. M., Jancarik, J., Yamaizumi, Z., Nishimura, S., Ohtsuka, E., and Kim, S.-H. (1990) *Proc. Natl. Acad. Sci. U.S.A. 87*, 4849−4853.
26. Milburn, M. V., Tong, L., deVos, A. M., Brünger, A., Yamaizumi, Z., Nishimura, S., and Kim, S.-H. (1990) *Science 247*, 939−945.
27. Krengel, U., Schlichting, I., Scherer, A., Schumann, R., Frech, M., John, J., Kabsch, W., Pai, E. F., and Wittinghofer, A. (1990) *Cell 62*, 539−548.
28. Schlichting, I., Almo, S. C., Rapp, G., Wilson, K., Petratos, K., Lentfer, A., Wittinghofer, A., Kabsch, W., Pai, E. F., Petsko, G. A., and Goody, R. S. (1990) *Nature 345*, 309−315.
29. Tong, L., de Vos, A. M., Milburn, M. V., and Kim, S.-H. (1991) *J. Mol. Biol. 217*, 503−516.
30. Privé, G. G., Milburn, M. V., Tong, L., de Vos, A. M., Yamaizumi, Z., Nishimura, S., and Kim, S.-H. (1992) *Proc. Natl. Acad. Sci. U.S.A. 89*, 3649−3653.
31. Franken, S. M., Scheidig, A. J., Krengel, U., Rensland, H., Lautwein, A., Geyer, M., Scheffzek, K., Goody, R. S., Kalbitzer, H. R., Pai, E. F., and Wittinghofer, A. (1993) *Biochemistry 32*, 8411−8420.
32. Scheidig, A. J., Franken, S. M., Corrie, J. E., Reid, G. P., Wittinghofer, A., Pai, E. F., and Goody, R. S. (1995) *J. Mol. Biol. 253*, 132−150.
33. Kraulis, P. J., Domaille, P. J., Campbell-Burk, S. L., Van Aken, T., and Laue, E. D. (1994) *Biochemistry 33*, 3515−3531.
34. Ha, J.-M., Ito, Y., Kawai, G., Miyazawa, T., Miura, K., Ohtsuka, E., Noguchi, S., Nishimura, S., and Yokoyama, S. (1989) *Biochemistry 28*, 8411−8416.
35. Hata-Tanaka, A., Kawai, G., Yamasaki, K., Ito, Y., Kajiura, H., Ha, J.-M., Miyazawa, T., Yokoyama, S., and Nishimura, S. (1989) *Biochemistry 28*, 9550−9556.
36. Campbell-Burk, S. (1989) *Biochemistry 28*, 9478−9484.
37. Campbell-Burk, S., Papastavros, M. Z., McCormick, F., and Redfield, A. G. (1989) *Proc. Natl. Acad. Sci. U.S.A. 86*, 817−820.
38. Yamasaki, K., Kawai, G., Ito, Y., Muto, Y., Fujita, J., Miyazawa, T., Nishimura, S., and Yokoyama, S. (1989) *Biochem. Biophys. Res. Commun. 162*, 1054−1062.
39. Redfield, A. G., and Papastavros, M. Z. (1990) *Biochemistry 29*, 3509−3514.
40. Schlichting, I., John, J., Frech, M., Chardin, P., Wittinghofer, A., Zimmermann, H., and Rösch, P. (1990) *Biochemistry 29*, 504−511.
41. Yamasaki, K., Muto, Y., Ito, Y., Wälchli, M., Miyazawa, T., Nishimura, S., and Yokoyama, S. (1992) *J. Biomol. NMR 2*, 71−82.
42. Muto, Y., Yamasaki, K., Ito, Y., Yajima, S., Masaki, H., Uozumi, T., Wälchli, M., Nishimura, S., Miyazawa, T., and

Yokoyama, S. (1993) *J. Biomol. NMR 3*, 165−184.
43. Campbell-Burk, S. L., Domaille, P. J., Starovasnik, M. A., Boucher, W., and Laue, E. D. (1992) *J. Biomol. NMR 2*, 639−646.
44. Miller, A. F., Papastavros, M. Z., and Redfield, A. G. (1992) *Biochemistry 31*, 10208−10216.
45. Miller, A. F., Halkides, C. J., and Redfield, A. G. (1993) *Biochemistry 32*, 7367−7376.
46. Hu, J.-S., and Redfield, A. G. (1993) *Biochemistry 32*, 6763−6772.
47. Campbell-Burk, S. L., and Van Aken, T. E. (1993) *Handb. Exp. Pharmacol. 108*, 213−231.
48. Yamasaki, K., Shirouzu, M., Muto, Y., Fujita-Yoshigaki, J., Koide, H., Ito, Y., Kawai, G., Hattori, S., Yokoyama, S., Nishimura, S., and Miyazawa, T. (1994) *Biochemistry 33*, 65−73.
49. Ikura, M., Kay, L. E., and Bax, A. (1990) *Biochemistry 29*, 4659−4667.
50. Miura, K., Inoue, Y., Nakamori, H., Iwai, S., Ohtsuka, E., Ikehara, M., Noguchi, S., and Nishimura, S. (1986) *Jpn. J. Cancer Res. 77*, 45−51.
51. Laue, E. D., Mayger, M. R., Skilling, J., and Staunton, J. (1986) *J. Magn. Reson. 68*, 14−29.
52. Grzesiek, S., and Bax, A. (1992) *J. Magn. Reson. 96*, 432−440.
53. Powers, R., Gronenborn, A. M., Clore, G. M., and Bax, A. (1991) *J. Magn. Reson. 94*, 209−213.
54. Marion, D., Driscoll, P. C., Kay, L. E., Wingfield, P. T., Bax, A., Gronenborn, A. M., and Clore, G. M. (1989) *Biochemistry 28*, 6150−6156.
55. Marion, D., Kay, L. E., Sparks, S. W., Tochia, D. A., and Bax, A. (1989) *J. Am. Chem. Soc. 111*, 1515−1517.
56. Skelton, N. J., Palmer, A. G., III, Akke, M., Kördel, J., Rance, M., and Chazin, W. J. (1993) *J. Magn. Reson., Ser. B 102*, 253−264.
57. Bonner, T. I., Kerby, S. B., Sutrave, P., Gunnell, M. A., Mark, G., and Rapp, U. R. (1985) *Mol. Cell. Biol. 5*, 1400−1407.
58. Bonner, T. I., Oppermann, H., Seeburg, P., Kerby, S. B., Gunnell, M. A., Young, A. C., and Rapp, U. R. (1986) *Nucleic Acids Res. 14*, 1009−1015.
59. Chuang, E., Barnard, D., Hettich, L., Zhang, X.-F., Avruch, J., and Marshall, M. S. (1994) *Mol. Cell. Biol. 14*, 5318−5325.
60. Kigawa, T., Muto, Y., and Yokoyama, S. (1995) *J. Biomol. NMR 6*, 129−134.
61. Studier, F. W., Rosenberg, A. H., Dunn, J. J., and Dubendorff, J. W. (1991) *Methods Enzymol. 185*, 60−89.
62. Kay, L. E., Torchia, D. A., and Bax, A. (1989) *Biochemistry 28*, 8972−8979.
63. Ghosh, S., Xie, W.-Q., Quest, A. F., Mabrouk, G. M., Strum, J. C., and Bell, R. M. (1994) *J. Biol. Chem. 269*, 10000−10007.
64. Ghosh, S., and Bell, R. M. (1994) *J. Biol. Chem. 269*, 30785−30788.
65. Brtva, T. R., Drugan, J. K., Ghosh, S., Terrell, R. S., Campbell-Burk, S., Bell, R. M., and Der, C. J. (1995) *J. Biol. Chem. 270*, 9809−9812.
66. Hu, C.-D., Kariya, K., Tamada, M., Akasaka, K., Shirouzu, M., Yokoyama, S., and Kataoka, T. (1995) *J. Biol. Chem. 270*, 30274−30277.
67. Drugan, J. K., Khosravi-Far, R., White, M. A., Der, C. J., Sung, Y.-J., Hwang, Y.-W., and Campbell, S. L. (1996) *J. Biol. Chem. 271*, 233−237.
68. Emerson, S. D., Waugh, D. S., Scheffler, J. E., Tsao, K.-L., Prinzo, K. M., and Fry, D. C. (1994) *Biochemistry 33*, 7745−7752.
69. Emerson, S. D., Madison, V. S., Palermo, R. E., Waugh, D. S., Scheffler, J. E., Tsao, K.-L., Kiefer, S. E., Liu, S.-P., and Fry, D. C. (1995) *Biochemistry 34*, 6911−6918.
70. Mott, H. R., Carpenter, J. W., Zhong, S., Ghosh, S., Bell, R. M., and Campbell, S. L. (1996) *Proc. Natl. Acad. Sci. U.S.A. 93*, 8312−8317.
71. Nassar, N., Horn, G., Herrmann, C., Scherer, A., McCormick, F., and Wittinghofer, A. (1995) *Nature 375*, 554−560.
72. Nassar, N., Horn, G., Herrmann, C., Block, C., Janknecht, R., and Wittinghofer, A. (1996) *Nat. Struct. Biol. 3*, 723−729.
73. Ponting, C. P., and Benjamin, D. R. (1996) *Trends Biochem. Sci. 21*, 422−425.
74. Mittal, R., Ahmadian, M. R., Goody, R. S., and Wittinghofer, A. (1996) *Science 273*, 115−117.
75. Neal, S. E., Eccleston, J. F., and Webb, M. R. (1990) *Proc. Natl. Acad. Sci. U.S.A. 87*, 3562−3565.
76. Rensland, H., Lautwein, A., Wittinghofer, A., and Goody, R. S. (1991) *Biochemistry 30*, 11181−11185.
77. Moore, K. J., Webb, M. R., and Eccleston, J. F. (1993) *Biochemistry 32*, 7451−7459.
78. Schweins, T., Geyer, M., Scheffzek, K., Warshel, A., Kalbitzer, H. R., and Wittinghofer, A. (1995) *Nat. Struct. Biol. 2*, 36−44.
79. Skinner, R. H., Bradley, S., Brown, A. L., Johnson, N. J., Rhodes, S., Stammers, D. K., and Lowe, P. N. (1991) *J. Biol. Chem. 266*, 14163−14166.
80. Wiesmüller, L., and Wittinghofer, A. (1992) *J. Biol. Chem. 267*, 10207−10210.
81. Brownbridge, G. G., Lowe, P. N., Moore, K. J., Skinner, R. H., and Webb, M. R. (1993) *J. Biol. Chem. 268*, 10914−10919.
82. Gutmann, D. H., Boguski, M., Marchuk, D., Wigler, M., Collins, F. S., and Ballester, R. (1993) *Oncogene 8*, 761−769.
83. Chung, H.-H., Benson, D. R., and Schultz, P. G. (1993) *Science 807*, 806−809.
84. Geyer, M., Schweins, T., Herrmann, C., Prisner, T., Wittinghofer, A., and Kalbitzer, H. R. (1996) *Biochemistry 35*, 10308−10320.
85. Smith, S. A., Levante, T. O., Meier, B. H., and Ernst, R. R. (1994) *J. Magn. Reson., Ser. A 106*, 75−105.
86. Kay, L. E., and Bax, A. (1990) *J. Magn. Reson. 86*, 110−126.
87. Brünger, A. T. (1992) *X-PLOR Version 3.1*, Yale University, New Haven, CT.
88. Nilges, M., Gronenborn, A. M., Brünger, A. T., and Clore, G. M. (1988) *Protein Eng. 2*, 27−38.

BI970296U